

# Journal of Materials Chemistry C

Accepted Manuscript



This is an *Accepted Manuscript*, which has been through the Royal Society of Chemistry peer review process and has been accepted for publication.

*Accepted Manuscripts* are published online shortly after acceptance, before technical editing, formatting and proof reading. Using this free service, authors can make their results available to the community, in citable form, before we publish the edited article. We will replace this *Accepted Manuscript* with the edited and formatted *Advance Article* as soon as it is available.

You can find more information about *Accepted Manuscripts* in the [Information for Authors](#).

Please note that technical editing may introduce minor changes to the text and/or graphics, which may alter content. The journal's standard [Terms & Conditions](#) and the [Ethical guidelines](#) still apply. In no event shall the Royal Society of Chemistry be held responsible for any errors or omissions in this *Accepted Manuscript* or any consequences arising from the use of any information it contains.



# Journal of Material Chemistry C

## ARTICLE

### Self-assembly of White-light Emitting Polymer with Aggregation Induced Emission Enhancement using Simplified Derivatives of Tetraphenylethylenet†

Received 00th January 20xx,  
Accepted 00th January 20xx

DOI: 10.1039/x0xx00000x

www.rsc.org/

Ezhakudiyan Ravindran,<sup>ab</sup> Elumalai Varathan,<sup>abc</sup> Venkatesan Subramanian,<sup>abc</sup> and Narayanasastri Somanathan<sup>\*abc</sup>

White-light emitting materials and devices have gained a great deal of interest and play an important role in the next generation solid-state lighting applications. The unique aggregation-induced emission (AIE) route offers a forthright solution to the bottle neck problem of aggregation caused quenching (ACQ) in the solid state. A significant fluorescence enhancement was realized by tailoring a new luminogen (2Z,2'Z)-3,3'-((9,9-dihexyl-9H-fluorene-2,7-diyl)bis(3,1-phenylene))bis(2-(4-bromophenyl)-3-phenylacrylonitrile) (FBPAN) based on AIE strategy, which exhibits yellow fluorescence with high quantum yield of 63.41%. Electroluminescence characteristics with maximum luminance, current and power efficiency of 16673 cd/m<sup>2</sup>, 9.32 cd/A and 5.88 lm/W, respectively were obtained for FBPAN. The white light emitting polymers were obtained by the copolymerization of 9,9'-dihexylfluorene host with FBPAN moiety as a covalent dopant. A bright white light emission with high quantum yield of 80.2% was obtained from the copolymer FBPAN 0.5, which contained 0.5% FBPAN. Importantly, the copolymers exhibit, an enhanced emission upon aggregation, even at low compositions of FBPAN. A careful inspection reveals that the enhanced emission in the solid state is due to the formation of "J-aggregates" with ordered supramolecular self-assembly. Interestingly, the copolymer FBPAN 0.5 exhibits unique ordered flower shaped self-assembly and significantly reduces the charge trapping due to balanced charge transport. As a result, bright and high efficient white light emission was achieved with Commission Internationale de l'Eclairage (CIE) coordinates of (0.32, 0.31) and maximum luminance, current and power efficiency of 13455 cd/m<sup>2</sup>, 7.56 cd/A and 5.32 lm/W, respectively. The copolymers possess very low turn-on voltage in the range of 1.5 to 3 V.

### Introduction

The more recent and emerging fields of organic and molecular electronics materials have resulted in the development of smart materials and devices that find various applications in the modern era. Among the materials developed light emitting diodes based on organic fluorophore/polymers are particularly important since the energy consumption in OLEDs is much less compared to that of conventional fluorescent light.<sup>1</sup> Specifically, white organic light emitting materials and devices (WOLED) have drawn massive interest in both scientific and

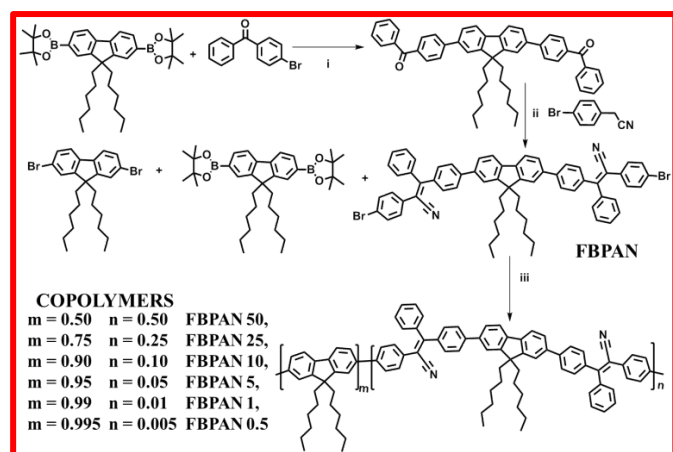
industrial communities and play an important role in the next generation solid state lighting applications.<sup>2,3</sup> The extensive progression of the materials, the simple device structure, and the light-extraction mechanisms have enabled tremendous advancement in WOLED efficacy over the recent years.<sup>4</sup> In general, for ideal white light emission, one can mix an appropriate ratio of three primary colors ((red, green and blue, (RGB)), or two complementary colors (yellow or orange and blue) to cover the entire visible spectral region (400–700 nm).<sup>5</sup> Diverse strategies towards realizing polymer white light emitting diodes (PWLEDs) such as single-layer polymer-blend system<sup>6</sup> and the multilayer-device system,<sup>7</sup> have been reported in both organic and organometallic chemistry. However, the aforementioned systems have several drawbacks: (i) the complications can arise if crystallization and the order change occur in the film morphology during device operation, (ii) The interfacial mixing of different layers (undesired energy transfer between the chromophores) and the intrinsic phase separation during long-term device function.<sup>8</sup> The above mentioned limitations can however be minimized if the devices are made with a single polymer emissive layer. White light emitting single-polymers (WLEPs) are of great interest in the field of

<sup>a</sup> CSIR-Central Leather Research Institute (CLRI), Polymer Laboratory, Adyar, Chennai, 600 020, India. \*E-mail: [nsomanathan@rediffmail.com](mailto:nsomanathan@rediffmail.com); Fax: +91-44-24911589; Tel: +91-44-24437189.

<sup>b</sup> CSIR-Network of Institutes for Solar Energy, Chemical Laboratory, CLRI, India.

<sup>c</sup> Academy of Scientific and Innovative Research (AcSIR), Anusandhan Bahavan, 2 Rafi Marg, New Delhi 110001, India.

† Electronic supplementary information (ESI) available: Detailed synthetic strategy and procedure for synthesis of monomer and copolymers. <sup>1</sup>H, <sup>13</sup>C, IR and MALDI mass spectrum of Monomer and <sup>1</sup>H and <sup>13</sup>C NMR spectra of copolymers, Computational details with other results of spectral and device properties are present in ESI. DOI: 10.1039/b000000x/.



**Scheme 1** Design and synthesis of AIEgen with derivatives of tetraphenylethylene based Yellow-emitting monomer (FBPAN) and Suzuki polymerization with 9,9'-dihexylfluorene done with varying feed ratios of FBPAN moiety. (i) Pd(pph<sub>3</sub>)<sub>4</sub>, K<sub>2</sub>CO<sub>3</sub> (2M), Toluene/Water reflux for 48 hrs. (ii) NaH/Benzene reflux for 3hrs. (iii) Pd(pph<sub>3</sub>)<sub>4</sub>, NaHCO<sub>3</sub> reflux for 72 hrs.

light-emitting devices, as they can offer numerous contrast advantages, such as simple device architecture, low cost device fabrication, and ease of scaling up without any problems by solution processing.<sup>9</sup> Recently, we reported polyfluorene (PF) based WLEPs, whose backbone was decorated with a yellow emitting moiety; these polymers showed aggregation induced emission enhancement (AIEE) and efficient electroluminescence with high brightness.<sup>10</sup>

Over the past few years, several groups including our's<sup>10,11</sup> have developed a number of luminogens with AIE characteristics as emitters to endeavor OLEDs. The conventional organic luminophores are flat molecules with discotic shapes, which give better emission when molecularly dissolved in polar solvent. These flat structures induce strong  $\pi$ - $\pi$  stacking interactions and thereby quench the emission intensity in solid state. This notorious phenomenon is called as aggregation caused quenching (ACQ).<sup>12</sup> ACQ or any non radiative processes in the solid state, are still bottleneck obstacles for researchers to acquire efficient luminescent materials. The phenomenon AIE or AIEE mechanism was coined for the first time by Tang et al., who demonstrated it with a series of siloles and showed that these molecules could emit efficiently in the solid state, although they are completely non-emissive in the solution.<sup>13,14</sup> The widely accepted mechanism for this AIE or AIEE phenomenon is restriction of intramolecular rotation (RIR),<sup>15</sup> and twisted intramolecular charge transfer (TICT)<sup>16</sup>. Moreover, hydrogen bond formation,<sup>17</sup> organic ion pair formation<sup>18</sup> and photo induced electron transfer<sup>19</sup> are also known to be operate in AIE or AIEE. Notably, the AIEE organic materials have received great attention in the field of OLEDs and the luminogens possess good emissive properties in the aggregate state. Till date, a variety of fluorophores with AIEE characteristics have attracted much interest in multifunctional platform to contrast applications in biological cell imaging, bio/chemo sensors and particularly optoelectronic devices.<sup>20</sup> Among the various AIE luminogens, tetraphenylethylene (TPE) holds a modest

molecular structure and shows a remarkable AIE effect with high fluorescence quantum yield.<sup>21</sup> However, systematic studies focusing on the AIEE moiety incorporated into the copolymers to get efficient white light emission, are still scarce. Hence, to explore the influence of AIE moiety on the solid state emissions of the polymer, we designed and synthesized a new and simple architecture of yellow emitting, (2Z,2'Z)-3,3'-((9,9-dihexyl-9H-fluorene-2,7-diyl)bis(4,1-phenylene))bis(2-(4-bromophenyl)-3-phenylacrylonitrile) (FBPAN) AIEE moiety. This AIEE active material retains the attractive properties of enhanced emission in the aggregate state. A series of copolymers were synthesized by palladium-catalyzed Suzuki cross-coupling polymerization of AIEE monomer with a blue host 9,9-dihexylfluorene (DHF), (Scheme 1). It is worth mentioning here that there have been limited reports on the white light emitting copolymers comprising of AIEE active unit, which enables fine tuning of the photophysical and electroluminescent properties of the resulting polymers.

## Results and discussion

### Optical properties of monomer and copolymers

The photophysical properties of the FBPAN monomer and copolymers were investigated in solution and thin film state. In the current study, various feed ratio of the FBPAN unit was introduced into the copolymers and are labeled as FBPAN 0.5, FBPAN 1, FBPAN 5, FBPAN 10, FBPAN 25, FBPAN 50. The characteristics absorption spectra of molecularly dissolved in diluted THF (solution) and aggregated species (thin film) were recorded, which are shown in Fig 1 (a) and (b), and the corresponding spectroscopic and dynamic decay data are summarized in Table 1. In solution, the monomer FBPAN showed absorption maximum at 361 nm with a molar absorptivity of  $1.91 \times 10^3$  dl g<sup>-1</sup> cm<sup>-1</sup>.

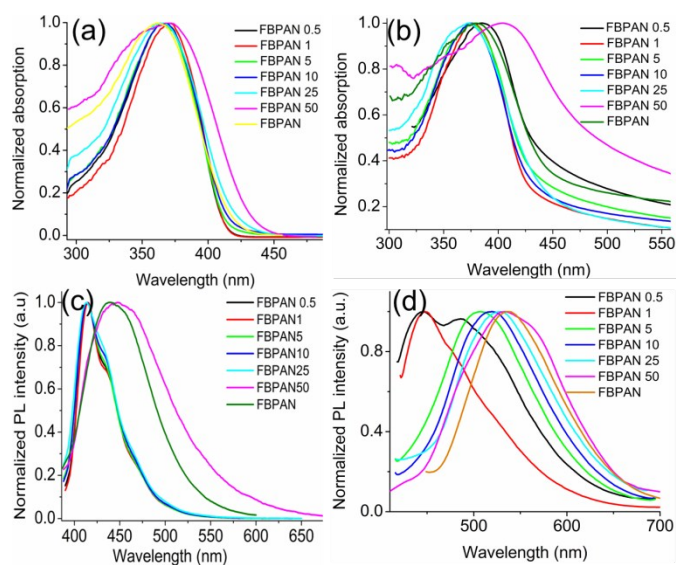


**Fig 1** (a), (b) Optical absorption spectra of FBPAN and copolymers in solutions and spun thin films; (c), (d) Optical emission spectra of monomer and copolymers in solution and spun thin films respectively. The concentration of solution is  $\sim 2.02 \times 10^{-4}$  g dl<sup>-1</sup>.

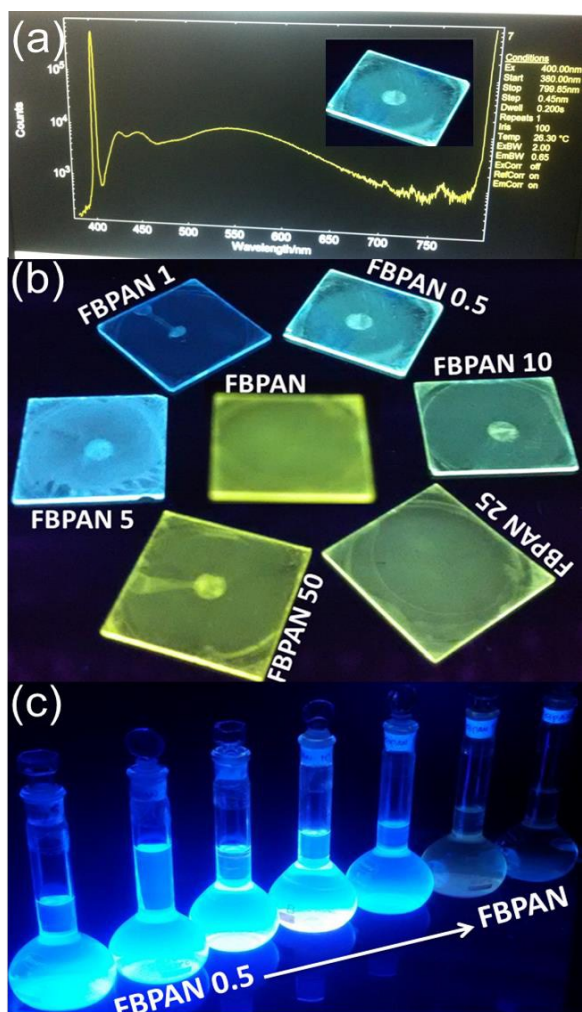


**Fig. 2** Photographs showing (a) absolute photoluminescence quantum yield spectrum of copolymer FBPAN 0.5 (inset FBPAN 0.5 film); (b) luminescence from spin coated thin films and (c) luminescence from THF solutions of copolymers under 365 nm irradiation.

The copolymers, however exhibited a slight red shift in absorption maxima with a concomitant spectral broadening, which is attributed to the spectral overlap of polyfluorene and FBPAN segments.<sup>22</sup> In thin film, the absorption spectrum of FBPAN was red shifted by 20 nm towards the longer wavelength compared to that of solution. Similar to the solution, the absorption spectrum of the copolymers was red shifted with associated spectral broadening as the composition of polymer was enriched with FBPAN. The absorption maximum of FBPAN 0.5 was observed at 385 nm while that of FBPAN 50 at 405 nm. So FBPAN 50 showed 20 nm red shifted in the absorption maximum compared to that of the lowest composition in this series (FBPAN 0.5) and 36 nm red shift to its solution spectrum. The former observation is attributed to the increased fraction of the yellow emitting FBPAN in the polymer backbone while the later to the strong aggregates in the condensed phase. Derivatives of fluorene are known to be good energy donors for Förster resonance energy transfer (FRET) because of their proper HOMO–LUMO energy levels and deserving absolute quantum yield in both solution and thin film state.<sup>23</sup> Hence, in the designed polymers, the middle

core of 9,9'-dihexylfluorene in FBPAN can act as effective support for the organization of acceptor unit along with conjugated copolymer backbone. When the THF solution of FBPAN and the copolymers was irradiated with a UV lamp (365 nm excitation), a very weak emission was observed. However, the FBPAN monomer and the copolymers are all converted into much strong emitters in their aggregated state (thin film) as shown **Fig 2(c)** (solution) and **(b)** (thin film). These results indicate that these copolymers have acquired AIEE characteristic owing to the presence of AIEE-active FBPAN moiety in the backbone and validates our design strategy. In order to verify the AIEE characteristics of copolymers we investigated the typical photoluminescence (PL) behavior in the solution and aggregate state.

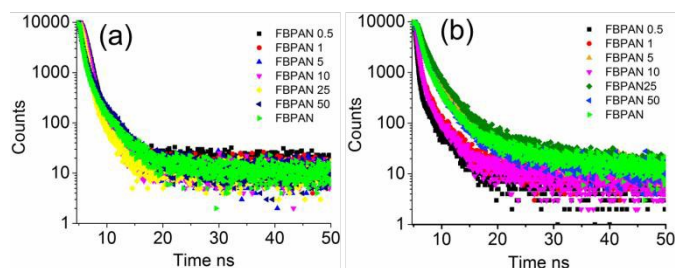
In solution state, the lowest composition of copolymers (FBPAN 0.5 – FBPAN 10) exhibited two emission maxima, centered at  $\sim 415$  and  $\sim 472$  nm respectively, corresponding to the emission of poly(9,9-dihexylfluorene)-2,7-diyl (DHFP)<sup>24</sup> and FBPAN unit as shown in **Fig 1(c)** and **Table 1**. Nevertheless, FBPAN 50 showed only one emission peak centered around 448 nm, which indicates that there is a partial resonance energy transfer between DHFP and FBPAN moiety.<sup>25</sup> The photoluminescence quantum yields (PLQY) of FBPAN 0.5, FBPAN 1, FBPAN 5, FBPAN 10, FBPAN 25, FBPAN 50 and FBPAN in oxygen-free THF are 63.9, 59.5, 62.2, 31.5, 16.0, 1.5 and 0.8 respectively, as shown in **Table 1**. Notably, the common decreasing trend of solution quantum yield clearly suggests that the increase in the fraction of an AIEE-active moiety in the composition of the copolymers reduces the fluorescence emission as anticipated.<sup>26,27</sup> This is pictorially represented in **Fig 2 (c)**.

In thin film, the normalized PL spectra of monomer and copolymers spectra are shown in **Fig 1 (d)**. The emission spectra of the films are in contrast to those of the solutions as expected. The emission spectra of all the copolymers, except FBPAN 0.5, showed only one peak in the range of 445–530 nm. The copolymer of FBPAN 50 exhibited a predominant emission at 530 nm, which is 85 nm red shifted in the emission maximum compared to that of the lowest composition in this series (FBPAN 0.5). The gradual bathochromic shift of the emission maximum is attributed to the self-quenching of the emission from fluorene segment and the concomitant energy transfer to the FBPAN segments<sup>21</sup> leading to predominantly long wavelength emission with enhanced quantum yield in thin film state as shown in **Fig 2 (b) and Table 1**. In addition, the energy transfer becomes significant with increasing the feed ratios of FBPAN moieties in thin film state lead to long wavelength emission. Interestingly the copolymer FBPAN 0.5 showed two characteristic emission peaks with high absolute photoluminescence quantum yield (PLQY) in thin film state originating from the polyfluorene segments and FBPAN segments. Nevertheless, the white light emitting copolymer FBPAN 0.5, (minimum composition of FBPAN units) controls the intensity of long wavelength emission and elicited dual emission at  $\sim 445$  nm and  $\sim 492$  nm with enhanced PLQY of 80.2% as shown in **Fig 1 (d)** and **Fig 2 (a)**. As a result, bright white light emission was observed for FBPAN 0.5 with PL CIE

**Table 1.** Spectral properties of monomer (FBPAN) and copolymers.

Polymers	<sup>a</sup> $\lambda_{\max}$ (Abs) (nm)		<sup>c</sup> $\lambda_{\max}$ (Emi) (nm)		<sup>d</sup> Fluorescence lifetime		<sup>e</sup> $\Phi_{\text{PL}}^{\text{SOL}}$	<sup>f</sup> $\Phi_{\text{PL}}^{\text{TF}}$
	Solution <sup>b</sup> ( $\epsilon$ )	Thin film (Exc)	Solution	Thin film (Exc)	Solution ( $\tau_1/\tau_2$ )	Thin film ( $T_1/T_2$ )		
FBPAN0.5	367 (1.81x10 <sup>3</sup> )	385	415, 472 (367)	445, 492 (385)	0.41/2.63	0.79/2.62	63.9	80.2
FBPAN 1	371 (1.84x10 <sup>3</sup> )	376	415, 471 (371)	448 (376)	0.45/2.97	0.80/3.28	53.5	68.3
FBPAN 5	364 (1.53x10 <sup>3</sup> )	377	414, 470 (364)	507 (377)	0.81/3.21	0.75/2.63	62.2	71.4
FBPAN 10	367 (1.68x10 <sup>3</sup> )	374	414, 474 (367)	520 (374)	0.98/3.06	0.75/2.74	31.5	59.0
FBPAN 25	366 (1.52x10 <sup>3</sup> )	374	415, 476 (366)	528 (374)	1.06/3.18	0.66/2.40	16.0	63.5
FBPAN 50	369 (1.05x10 <sup>3</sup> )	405	448 (369)	530 (405)	1.16/3.27	0.76/2.78	1.5	67.4
FBPAN	361 (1.91x10 <sup>3</sup> )	381	439 (361)	536 (381)	1.73/2.95	0.68/2.75	0.8	63.4

<sup>a</sup> $\lambda_{\max}$  (Abs), absorption maxima for solutions and thin films in nm; <sup>b</sup>( $\epsilon$ ), extinction coefficient in dL g<sup>-1</sup> cm<sup>-1</sup>. <sup>c</sup> $\lambda_{\max}$  (Emi), emission maxima for solutions and thin films in nm. <sup>d</sup>  $\tau_1/\tau_2$  and  $T_1/T_2$ , lifetime of different decay channels from fluorescence lifetime experiment in ns for solutions and thin films; <sup>e</sup> $\Phi_{\text{PL}}^{\text{SOL}}$ , The solution absolute PL quantum yields were measured using an integrating sphere; <sup>f</sup> $\Phi_{\text{PL}}^{\text{TF}}$ , The thin film absolute PL quantum yields were measured using an integrating sphere.

**Fig 3** (a) and (b) fluorescence lifetime decay of copolymers in solutions and thin films

coordinates of (0.30, 0.31), which is quite close to those of pure white light (0.33, 0.33). Moreover, the energy transfer becomes more efficient as we fine-tune the fraction of FBPAN moiety and high emission of FBPAN moiety leads to gradual redshift in thin film for all copolymers.<sup>28</sup>

The fluorescence life time decay experiments of the monomer and copolymers in solutions and thin films were carried out to identify the significance of aggregation on the dynamics decay of the excited state<sup>29</sup> and the corresponding decay profiles are shown in **Fig 3 (a)** and **(b)**. The monomer of FBPAN when monitored and the aggregates exhibited biexponential decay ( $\chi^2 = 1.09$ ) with life time values of 1.73 ns (32.05%) and 2.95 ns (67.95%) in solution; the thin film also shows biexponential decay ( $\chi^2 = 1.16$ ) with life time values of 0.68 ns and 2.7 ns and the corresponding amplitudes are 41.25% and 58.75% respectively. In order to quantify the average fluorescence life time of the copolymers, we investigated their fluorescence decay profiles in solution (THF). It is observed that the copolymers with low composition of FBPAN, such as FBPAN 0.5 through FBPAN 10, underwent ultrafast decay with life time < 1 ns and the obtained results are analogous to DHFP. On the contrary, the copolymers FBPAN 25, FBPAN 50 and FBPAN with high content did not show ultrafast decay ( $\tau_1 > 1$  ns). The above result are convincing that the copolymer with high content of fluorene is

more emissive, whereas high content of FBPAN containing copolymers is weakly emissive in THF solution. The lifetime decay of these copolymers linearly increased while increasing the content of FBPAN and the corresponding data are compiled in **Table 1**. In thin film, all the copolymers elucidate short lived and long lived species in the range of nano second. However, in thin film while increasing the feed ratios of monomer the percentage distribution of the decay channels found to be drastically decreased.

#### Study of aggregation induced emission enhancement

A large number of AIE luminogens enclosing cyano groups have been established.<sup>24</sup> Cyano group has been widely used as a functional unit in the architecture of optical functional materials. In the present study, we carefully examined the photo physical properties of monomer and copolymers. To investigate the AIEE traits of monomer and copolymers, UV-visible and fluorescent behaviors were studied through addition of a non-solvent such as water into the solution of fluorophore in good solvent. The absorption spectra of FBPAN upon addition of water to its THF solution showed very little change and a slight red shift was observed along with a spectral broadening **Fig S13 (g) (+SI)**. This phenomenon is well reported in literature for D-A luminogens and is attributed to twisted intra molecular charge transfer (TICT) state. In addition, we carried out the Lippert–Mataga study with different polarity of the solvent to confirm the TICT effect as shown in **Figure S11 (+SI)**.<sup>30</sup> The AIEE characteristics of the monomer FBPAN was investigated in THF-water mixture with varying amount of water fractions ( $f_w$ ) as shown in **Fig 4 (a)**. The monomer FBPAN shows very weak emission maxima at 416 nm, when molecularly dissolved in THF. The fluorescence intensity was found to decrease with increasing  $f_w$ , which is attributed to the increasing polarity of the medium that facilitates stabilization of charge transfer state by micro-

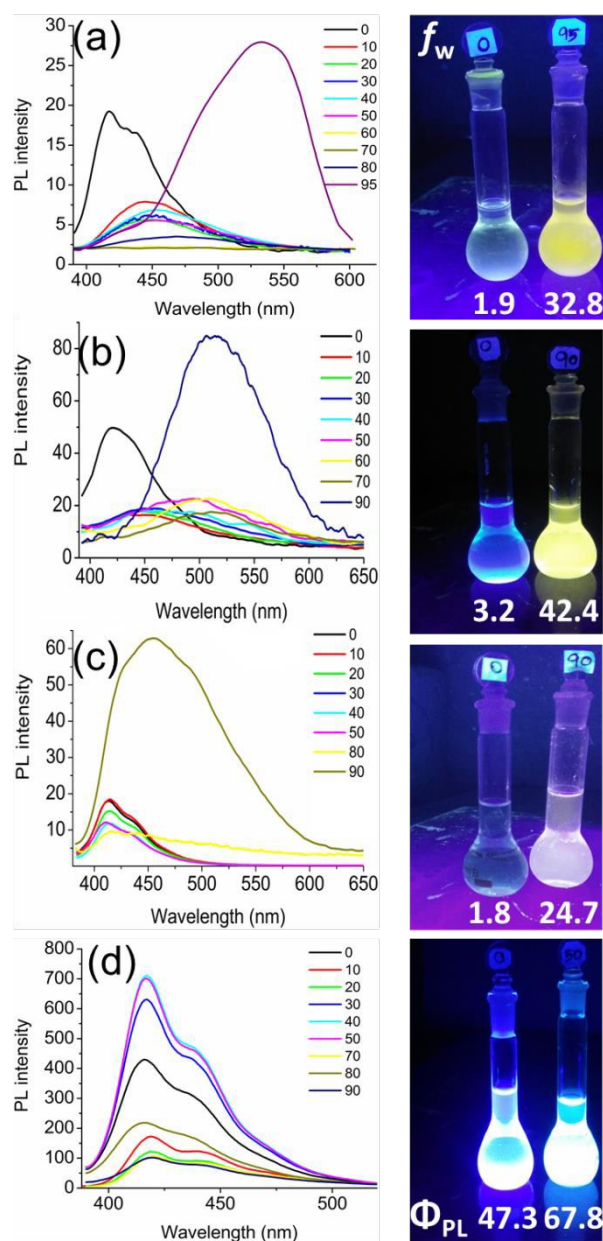


**Fig 4** (a) PL spectra of FBPAN monomer in THF and water mixtures with different water fractions ( $f_w$ ); Concentration:  $4 \times 10^{-4}$  g/dl; Excitation wavelength: 439 nm. (b), (c) and (d) are PL spectra of copolymer FBPAN 50, FBPAN 25 and FBPAN 0.5. Enclosure in right are the corresponding luminescence photographs taken under 365 nm UV irradiation, top and bottom of those UV irradiation pictures shows water fractions ( $f_w$ ) (in %) and absolute PL quantum yield (in %) respectively.

environment.<sup>31</sup> In other words, In THF and water mixtures with different  $f_w$ , FBPAN monomer shows TICT at  $f_w$  lower than 80% and AIE property at higher  $f_w$  due its restricted intramolecular rotation in aggregate state. However, at 80% of  $f_w$ , the fluorescence intensity increased sharply with a concomitant red shift of the emission maximum and reached highest intensity when  $f_w = 95\%$ . The emission maximum for 95%  $f_w$  (high  $f_w$ ) in solution was observed at 534 nm, which is 118 nm red shifted compared to its pure THF emission maximum. This offers further evidence of nano aggregate formation in THF-water mixtures with highest percentage of  $f_w$ .<sup>32</sup> The

mechanistic understanding of FBPAN monomer (AIEE active) having the molecular architecture of one conjugated stator carrying multiple aryl peripheral rotors with strong electron withdrawing group, which attribute to the formation of “J-aggregates” and restrictions of intra molecular rotation upon aggregate, induces the emission enhancement in aggregate states.<sup>33</sup> In order to determine the AIEE characteristics of FBPAN, the absolute photoluminescence quantum yield (PLQY) was measured through integrating sphere and dynamic light scattering measurements were recorded in solutions of FBPAN in different THF-water mixtures. The PLQY of FBPAN in pure THF is as low as 1.9% (**Fig 4 (a)**) and the corresponding hydrodynamic radius (Rh) is 92.64 nm as shown in **Fig 5 (a)** and **Fig S15 (†SI)**. However, the PLQY is 32.8%, when  $f_w$  reaches 95% (**Fig 4 (a)**) and the corresponding results from DLS experiment elucidate the presence of a broad peak at 533 nm (100%) (**Fig 5 (a)**). This indicates that the formation of aggregate thus induced emission enhancement; in additional words, FBPAN is undeniably AIEE active.<sup>34</sup> The UV illuminated photographs of FBPAN in pure THF (0%  $f_w$ ) and 95%  $f_w$  as shown in **Fig 4 (a) (in right)** clearly demonstrate the weak and strong emissions of the molecularly dissolved and aggregated species of FBPAN.

A similar AIEE behavior was also observed for the copolymers of FBPAN 50, FBPAN 25, due to the highest content of AIEE-active FBPAN unit present in that copolymer backbone as shown in **Fig 4 ((b) and (c))**. For this case a very weak PL intensity in pure THF solution for the reason that, derivatives of tetraphenylethylene containing phenyl rings in the side-chain of the copolymers can still rotate to some extent in solution, which decays the excitation energy. On the other

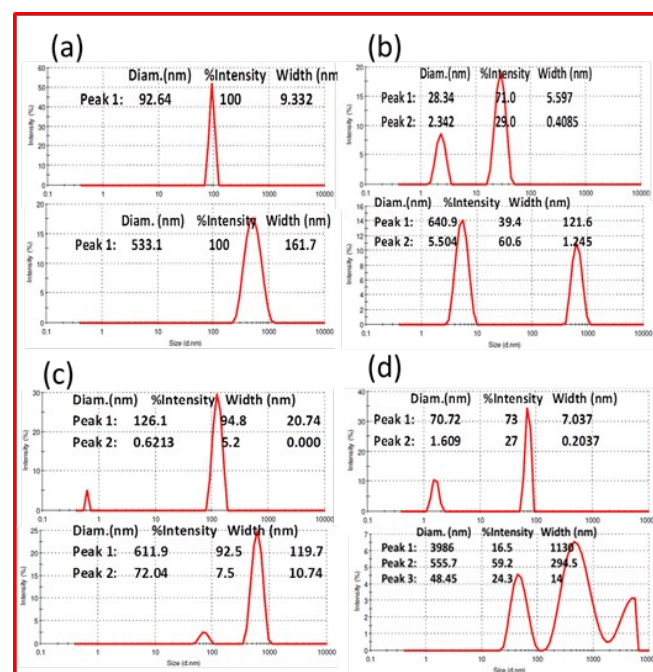


**Fig 5** (a), (b), (c) and (d) are DLS traces of monomer FBPAN and copolymers of FBPAN 50, FBPAN 25 and FBPAN 0.5 in the condition of initial and aggregated states.

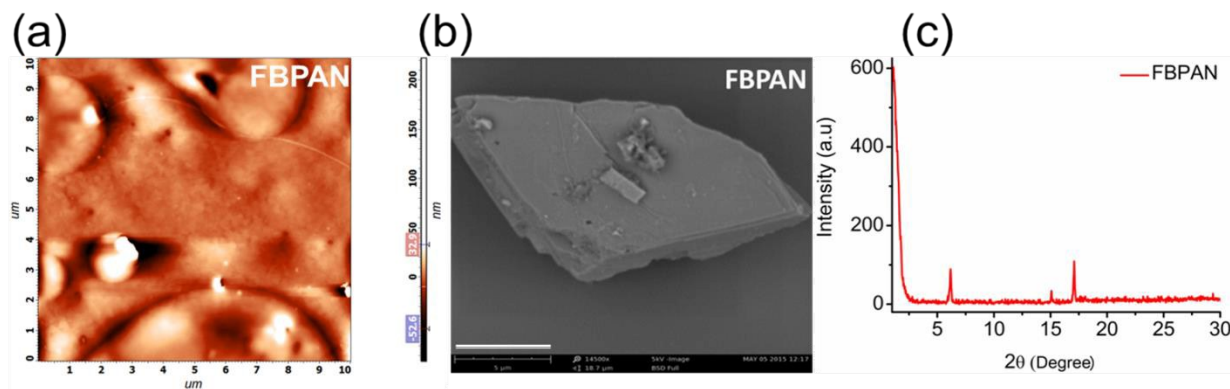


Fig 6 (a) and (b) AFM and SEM micrograph (scale bar for SEM image is 5  $\mu\text{m}$ ) of spun thin films from chloroform solution of FBPAN on ITO substrate (c) GIXRD trace of FBPAN in thin film.

hand, the restriction of intramolecular rotation (RIR) is often increased in the aggregate state, which blocks the nonradiative processes of the copolymers and improves the emission intensity in the aggregates.<sup>35</sup> The emission intensity was found to decrease initially and further gradual emission enhancement with bathochromic shift was observed up to  $f_w$  90% (maximum content of  $f_w$ ) in THF- water mixtures. The result of bathochromic shift in emission compared to that in respective molecularly dissolved pure THF, indicates that the formation of “J-aggregates” that induces emission intensity in the aggregates state. The PLQY for aggregates is 42.4% and 24.7%, which is 13 and 14 fold higher than that of pure THF solution (before addition of water) and the corresponding DLS measurements showed an intense and broad peak at Rh value of 641 and 612 nm, respectively and low intensity peak at 5.5 and 72.04, nm respectively for FBPAN 50 and FBPAN 25 as shown in **Fig 5 (b)** and **(c)**. The copolymers FBPAN 10, FBPAN 5 and FBPAN 1 showed one intense peak, which is centered at  $\sim$  415 nm attributed to fluorene segment emission. Upon addition of water into their pure THF solution, the PL intensity decreased up to the  $f_w$  at 70%, which is characteristic of emission quenching due to the aggregates of fluorene segment. However, increasing the  $f_w$  led to partial emission enhancement with a concomitant red shift as shown in **Fig S14 (†SI)**. Excitingly, the white light emitting copolymer of FBPAN 0.5 showed an enhanced emission with maximum intensity at 50% water in THF and the PL intensity reached 10 fold higher than that in pure THF. Significant enhancement in fluorescence absolute quantum yield was observed for  $f_w = 50\%$  (67.8%) and dynamic radii of FBPAN 0.5 show Rh value at 555 nm and it was broadened as shown in **Fig 4 (d)** and **5 (d)**. In addition to that result, a very narrow red shifted absorption bands with increasing percentage of water content. The bluish-white emission observed in aggregates of FBPAN 0.5 is in contrast, to white emission observed in thin film state. The above results clearly indicate the formation “J-aggregates”, which induce the PL intensity of FBPAN 0.5. The above elucidations clearly specify that the AIEE property of FBPAN was very effective even when feed ratio was as low as 0.5%. These verdicts confirm the presence of AIEE behavior even in low content of FBPAN in the copolymers. The results were verified by a control experiment, where PL spectra of poly 9,9-

dihexylfluorene (DHFP) was studied in different THF-water mixtures as reported in our previous report.<sup>36</sup>

#### Investigation of supramolecular assembly

In the past decades, architecture of supramolecular self-assembled materials for OLEDs and LCDs have gained a lot of attention and have been extensively studied.<sup>37,38</sup> In general, supramolecularly designed polymers generate hierarchically well-ordered structures and properties through self-assembly, which has received varied interest in the fields of sustainable energy and medicine.<sup>39-41</sup> In addition, formation of “J-aggregates” is of significant importance as it leads to well-defined supramolecular self-assembly and increased PLQY in both solution and solid state.<sup>42</sup> Atomic force micrographs (AFM) and the morphological features were correlated with the grazing incidence X-ray diffraction (GIXRD) analysis. The FBPAN monomer and copolymer were studied on films deposited on ITO substrates to decrypt more details of the intermolecular interactions. As depicted in **Fig 6 (c)**, FBPAN displays, sharp diffraction with replicating well crystalline character in nature. The intense degree of reflection ( $2\theta$ ) at 6.18 and 17.17°, corresponds to the ‘d’ spacing’s of 14.36 and 5.16 Å respectively. Another less intense reflection observed 15.08°, corresponds to the ‘d’ spacing of 5.86 Å; these findings suggests that some crystalline order maintaining in the molecular structure.<sup>43</sup> This means that the observed degree of reflection for FBPAN monomer can be permitted to the crystallinity of the spun thin film. The SEM and AFM analysis also supported the crystalline nature of the monomer as shown in **Fig 6 (a)** and **(b)**. The synthesized copolymers show highly ordered hallow spherical hierarchical supramolecular self-assemblies of micro scale morphologies, which contribute to overall functionality of improved device performance.<sup>44</sup> The resulting supramolecular architectures consisting of well-ordered morphology for all copolymers contains different feed ratios of FBPAN monomer unit in the backbone as evidenced by SEM and AFM analyses as shown in **Fig 7 (a)** and **Fig S16 (†SI)**. It is clear from the above discussion that the morphological topographies varied as the feed ratios of the FBPAN units changed in the polymeric backbone. The copolymer of FBPAN 50, FBPAN 25, FBPAN 10 (high feed ratios of FBPAN units) showed uniform hallow spherical hierarchical

supramolecular self-assemblies. Surprisingly, we noticed that the self-assemblies of white light emitting copolymer FBPAN 0.5 illustrated well defined "Flower shaped supramolecular self-assemblies (FSSS)" structure in spun thin films. The above observations are summarized using a schematic illustration in Fig 8. Furthermore, the FSSS structures were disturbed in the case of FBPAN 5 and FBPAN 1. This finding clearly indicates that the FBPAN monomer manifests the hierarchical assembly to the main chain of the copolymers. As expected the GIXRD pattern of the copolymers with low FBPAN content was similar to that of DHFP. However, GIXRD pattern completely changed

when the feed ratio is above 5% (i.e., above FBPAN 5). A remarkable changes were observed in AFM morphology for white light emitting copolymer of FBPAN 0.5, which can be correlated with scattering at  $2\theta = 5.93^\circ$  corresponding to the 'd' spacing of  $14.9 \text{ \AA}$ , which is greater than that of experimental value for  $\beta$ -phase of dialkyl fluorene moieties (characteristically observed at  $10.8 \text{ \AA}$ ).<sup>45</sup> In addition to the above reflection, a broad and intense diffractogram was observed for copolymer FBPAN 0.5 with reflection at  $2\theta = 19.85^\circ$  ( $4.5 \text{ \AA}$ ) corresponding to the amorphous hallow phase that is characteristic of fluorene polymers.<sup>46</sup>

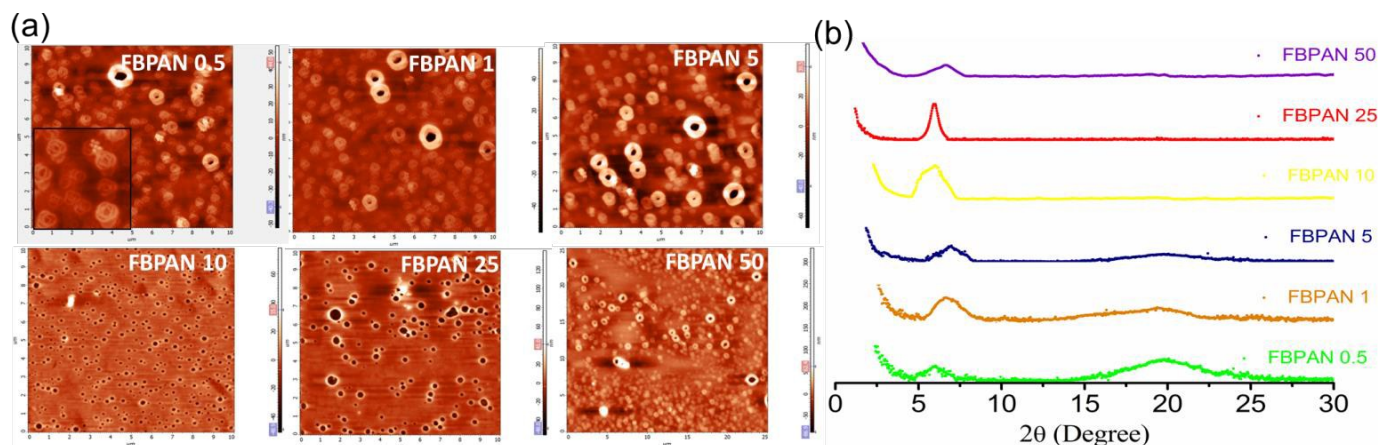


Fig 7 (a) Typical AFM micrographs of synthesized copolymers (b) Corresponding GIXRD pattern of the synthesized copolymers.

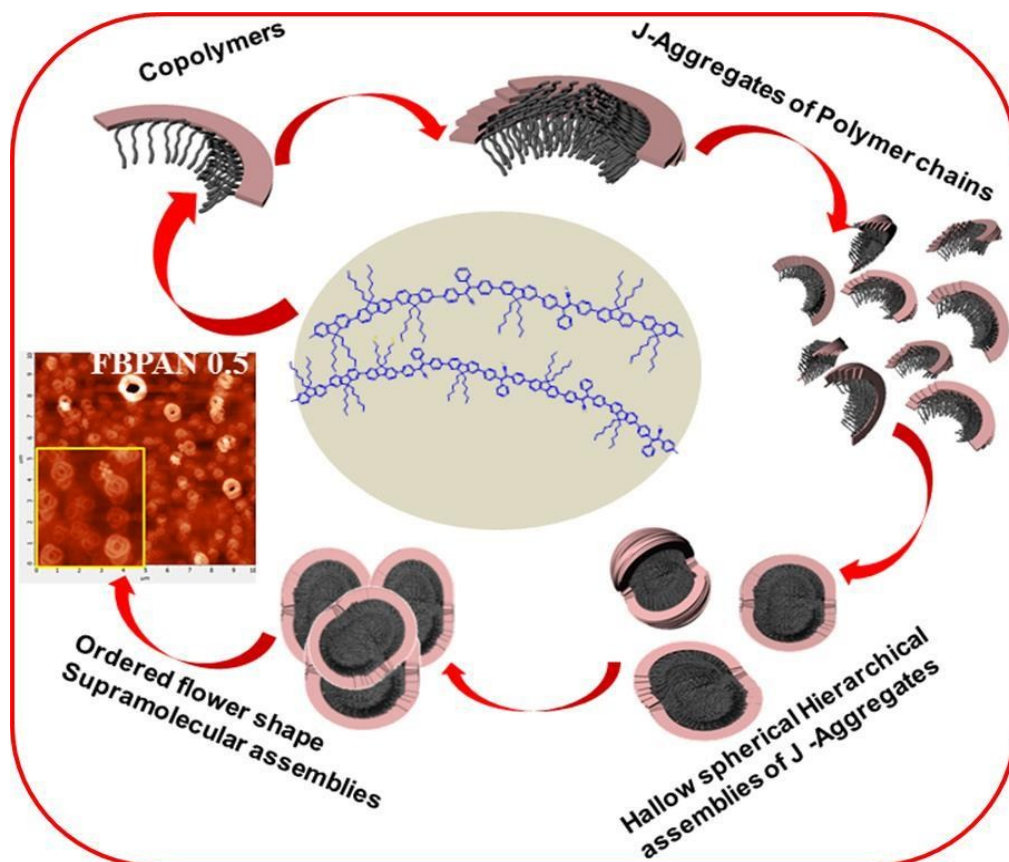


Fig 8 Structure and proposed schematic representation of J-aggregated ordered supramolecular self-assemblies of copolymers correlated with AFM morphology.

However, the characteristic reflection of  $2\theta$  values at 6.7 and 6.9° was also observed for the FBPAN 1 and FBPAN 5 with low feed ratios of FBPAN, respectively and the corresponding 'd' spacings are 13.2 and 12.8 Å which indicate a characteristic metastable  $\beta$ -phase accountable for enhanced quantum yield and thus justifying the high quantum yield for all copolymers in thin film state.<sup>47</sup> The FBPAN monomer shows sharp and intense degree of reflection at  $2\theta = 6.18^\circ$  corresponding to the 'd' spacing of 14.36 Å; however, broader reflection was observed in the case of FBPAN 50, FBPAN 25 and FBPAN 10 at  $2\theta$ , 6.68°, 5.93°, 6° respectively and the corresponding 'd' spacing of 13.22 Å, 14.89 Å, 14.72 Å. Notably, the typical amorphous hallow vanished in case of high feed ratios of FBPAN present in the copolymers. It is probable that the composition of FBPAN units in the 9,9-dihexylfluorene backbone induces a change in the supramolecular self-assemblies of the polymer chain. As a result, reduced feed ratios of FBPAN moieties can visualize the ordered flower shape supramolecular self-assemblies. So exhaustive understanding through AFM, SEM and GIXRD analyses revealed well crystalline order for FBPAN monomer, which is totally in contrast to that of copolymers as shown in Fig 6, 7 (a) and Fig S16 (†SI).

#### Structure of single polymer white OLEDs

A simple architecture of single polymer white organic light-emitting device (WOLED) reported here, has the device active layer, a solution-processed organic thin films, sandwiched between two charge-injecting contacts as shown in Fig 9. The external bias voltage is applied through an indium tin oxide (ITO) coated glass, which acts as an anode and Al that acts as cathode. The fabricated device is Al/Emissive polymer/PEDOT:PSS/ITO. In a typical device fabrication, an approximately 70-100 nm thick layer of poly (ethylenedioxythiophene): poly (styrene sulfonic acid) (PEDOT: PSS), which acts as hole transporting layer was deposited on an ITO substrate. Then the copolymers of various composition of FBPAN, which was coated on PEDOT:PSS layer with thickness of 100 – 115 nm acts as an emissive layer shown in Fig 9 by using a spin-coating procedure that has been described previously.<sup>48</sup> Finally a thin film of Al was coated to complete the device architecture.

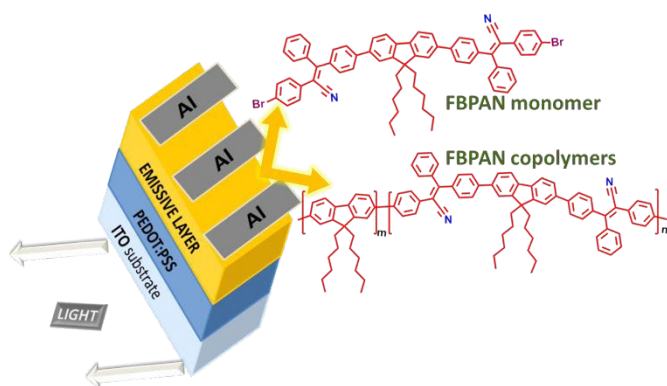


Fig 9 Architectures of the single emissive layer electroluminescent OLED device configuration with chemical structure of emissive monomer and copolymers.

#### Electrochemical and Single layer polymer device characteristics

Electrochemical properties and energy levels of monomer and copolymers are examined by cyclic voltammetry. In a typical three electrode system platinum disc, platinum wire and Ag/AgCl were used as working, counter and reference electrodes respectively. The cyclic voltammetry experiments were done with a thin film of copolymers using tetra-n-butylammoniumhexa-fluorophosphate ((Bu<sub>4</sub>N)PF<sub>6</sub>) (0.1 M) as supporting electrolyte in acetonitrile. All the copolymers exhibited quasi-reversible oxidation and reduction. The HOMO and LUMO energy levels of the copolymers were calculated using the empirical formula,

$$EHOMO = - (4.8 + E_{\text{oxdn onset}}) \text{ eV and}$$

$$ELUMO = - (4.8 + E_{\text{rdxn onset}}) \text{ eV}$$

and the corresponding datas are provided in Table S2 (†SI). The data clearly suggest that the band gap of the copolymers decreases as the fraction of FBPAN is increased. This apparently due to the addition of longer wavelength absorbing component of FBPAN in the copolymer backbone, which shifts the onset of absorption to higher wavelength and hence results in band-gap reduction. The energy level diagrams for the monomer and copolymers are depicted in Fig 10 (b). In the

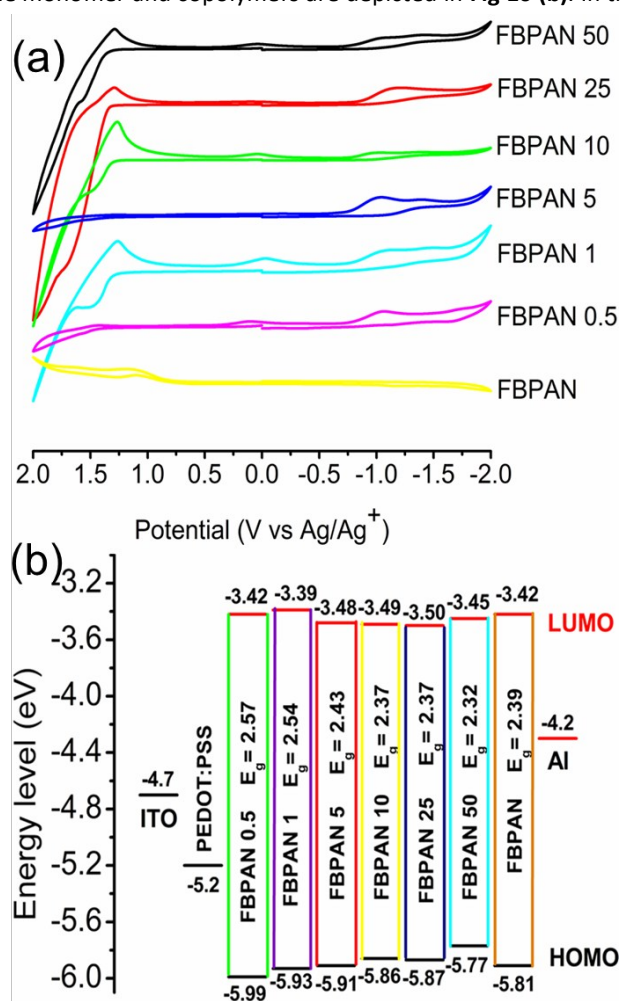
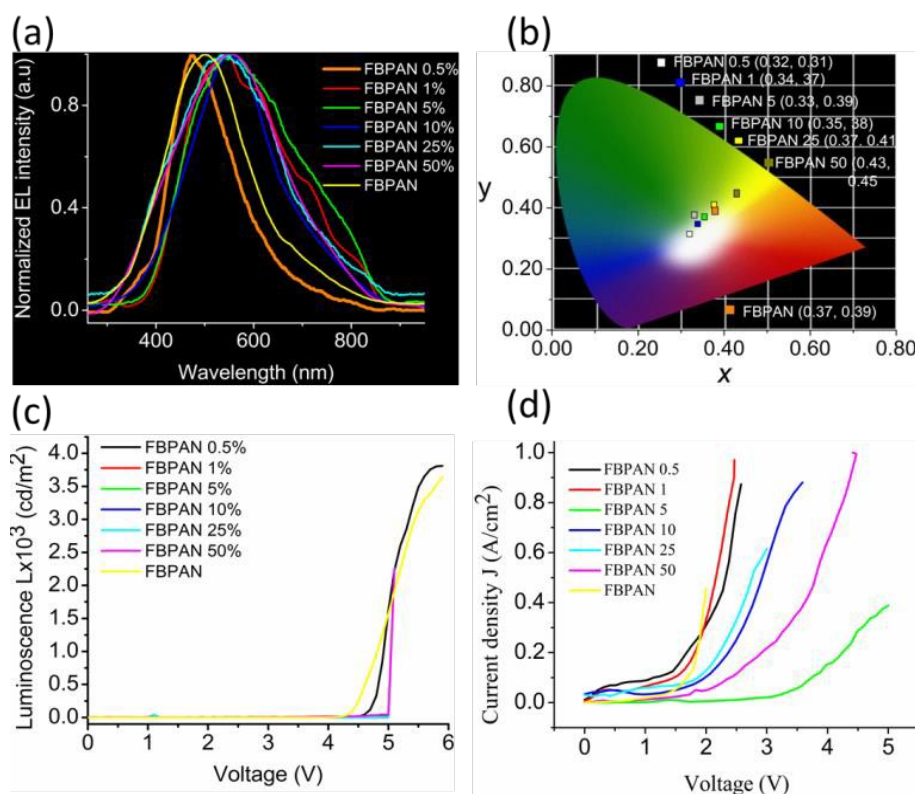


Fig 10 Energy level of the FBPAN monomer and copolymers. (a) Cyclic Voltammograms of the FBPAN monomer and copolymers. (b) Corresponding energy level diagram of the FBPAN monomer and copolymers.



**Fig 11** EL Performance of the single-layer OLEDs. (a) EL spectra of FBPAN monomer and copolymers; (b) Commission Internationale de l'Éclairage (CIE) chromaticity coordinates of the FBPAN and copolymers; (c) and (d) are the current density–voltage (J–V) and luminescence–voltage (L–V) plots of OLEDs for FBPAN monomer and copolymers

case of monomer FBPAN the energy offset for the hole injection is 0.61 eV, while that for electron injection is 0.78 eV. This implies that FBPAN constitutes holes as majority charge carriers leading to imbalance in charge injection. This shows that FBPAN could act as a trap for electrons.<sup>49</sup> the energy offset for the copolymers was investigated closely and it was found that FBPAN 0.5 showed a hybrid character of energy level, which are intermediate between those of dialkyl fluorene and FBPAN monomer. The LUMO energy level of this led to the balanced hole and electron injection barrier of 0.78 eV and 0.79 eV, which guarantees the equal charge injection and improved device efficiency. The LUMO energy level of FBPAN is same as that of the monomer (ELUMO = -3.42 eV), while the HOMO energy level is pushed deeper at -5.99 eV. However, other polymers exhibited slight deviation from balanced charge injection and the pertinent data are compiled in **Table S 2 (†SI)**

It is worth mentioning here that many fluorene based copolymers developed for highly efficient PWOLED exhibited charge imbalance with irregular charge injection, which led to the mismatch of EL and PL spectra.<sup>50(a)</sup> Such detrimental phenomenon was also observed for other white light emitting single polymers containing the dopant unit both in the main and side chains<sup>50(b)</sup> It is therefore very important to develop PWOLED with balanced charge carrier and also the PL and EL spectra should match in order to confirm that the same species is formed during the excitation through optical and electrical means.<sup>51</sup>

In order to investigate the electroluminescent device properties FBPAN monomer and the copolymers, were used to fabricate OLEDs with device configuration of ITO/PEDOT:PSS/polymer/Al by solution processing. The active emissive layer (polymers) sandwiched between two electrodes and PEDOT:PSS was chosen as a hole transporting layer. The monomer exhibited yellow EL while all the copolymers, except FBPAN 0.5 and FBPAN 1, showed yellow emission along with a spectral broadening. This result shows that incorporation of FBPAN to the polyfluorene backbone shifts the EL to the lower energy and also covering the entire visible region from 400 to 700 as shown in **Fig 11(a)** and their CIE coordinates values are presented in **Fig 11(b)**.

**Figure 11(a)** shows the EL spectrum of devices made from the FBPAN monomer and copolymers FBPAN 0.5, FBPAN 1, FBPAN 5, FBPAN 10, FBPAN 25, FBPAN 50. The EL spectrum of FBPAN was perceived to be broader than the PL spectrum, which can be attributed to the formation of electromer/excimer<sup>52</sup> and the copolymers show appropriate red shift with spectral broadening while increasing the feed ratio of the FBPAN content. The device properties of FBPAN elucidate the maximum luminance, current and power efficiencies are 16673  $\text{cd/m}^2$ , 9.32  $\text{cd/A}$  and 5.88  $\text{lm/W}$ , respectively.

In order to perceive highly efficient white electroluminescence, the device with copolymer FBPAN 0.5 was fabricated. The device exhibited pure white light emission with Commission Internationale de l'Éclairage (CIE) coordinates of (0.32, 0.31), which is very close to pure white light (0.33,0.33) with a very low turn on voltage of 1.4 V (**Fig 11(b) and (d)**). The maximum luminance of the white OLEDs fabricated from FBPAN 0.5 was found to be 13455  $\text{cd/m}^2$  at 9 V with maximum current and power efficiencies of 7.8  $\text{cd/A}$  and 5.9  $\text{lm/W}$ , respectively (**Fig 11(c), (d) and Table S 2 (†SI)**). As depicted in **Fig 11(a)**, a close view of EL spectrum of copolymers showed a yellow emission for FBPAN 50 and FBPAN 25 with a CIE coordinate of (0.43, 0.45) and (0.37, 0.41), respectively and displayed a maximum luminous efficiency of 8.33, 5.33  $\text{lm/W}$  and corresponding power efficiency found to be 9.12, 6.88  $\text{cd/A}$ , respectively with a low turn on voltage of  $\sim 1.7$  V. The maximum luminance observed for the copolymers FBPAN 50 and FBPAN 25 are 17342 and 10432  $\text{cd/m}^2$ , respectively as shown in **Table S2 (†SI)**. These studies again support our design strategy that increasing the FBPAN content in the copolymers backbone, successfully cover the entire visible region and produce efficient white light emission, through an enhanced Forster energy transfer from blue emitting polyfluorene segments to the yellow emitting core.<sup>53</sup>

The improved device performance of OLEDs with FBPAN 0.5 as the emissive layer can be attributed to the energy transfer from higher energy fluorene segments to lower energy of FBPAN segments. The EL and PL deconvolution spectra of FBPAN 0.5 are shown in (Fig S17 (c) (†SI)). The PL emission deconvoluted into two components with blue and yellow with the corresponding peaks at 435, 491 and 492 nm, respectively (Fig S17 (a) (†SI)). Interestingly, the EL deconvoluted spectrum of FBPAN 0.5 showed small red shifted peak maxima at 501 and 564. By scrutinizing carefully the EL and PL deconvolution spectra of the white light emitting copolymer FBPAN 0.5, it is found that they match very closely and the relative emission intensity between the higher energy blue host and lower energy of the covalent dopant in the EL spectra is similar to that in their PL spectra Fig S 13 (b) (†SI).

#### Theoretical studies on monomer and copolymers

Density functional theory (DFT) and time dependent density functional theory (TDDFT) approaches have been used to characterize electronic structure of the copolymers. The computational details are given in the supporting information. Optimized geometries of the model systems are shown in Fig S18 (†SI) The calculated electron density distributions of frontier molecular orbitals (FMO) are depicted in Fig 12. It is clear from Fig 12 that, all the model systems exhibit clear charge separated state. Close analysis of these orbitals reveals that the HOMO is predominantly localized on the fluorene unit and the LUMO is concentrated on the 2-(4-bromophenyl)-3,3-biphenylacrylonitrile unit. Hence, this feature confirms there is an intramolecular charge transfer (ICT) transition between the fluorine and 2-(4-bromophenyl)-3,3-biphenylacrylonitrile units. The calculated vertical excitation energies for monomer and oligomer using TDDFT approach are listed in Table 3. It can be noted from the table calculated values shows that the calculated spectral properties of the both monomer and oligomer are in close agreement with the experimental values. For the monomer FBPAN, the maximum peak is predicted to be at 362 nm ( $f=1.2629$ ), which arises from HOMO-1 to LUMO transition. In co- monomer, the maximum absorption peak is found to be at 349 nm ( $f = 0.9170$ ).

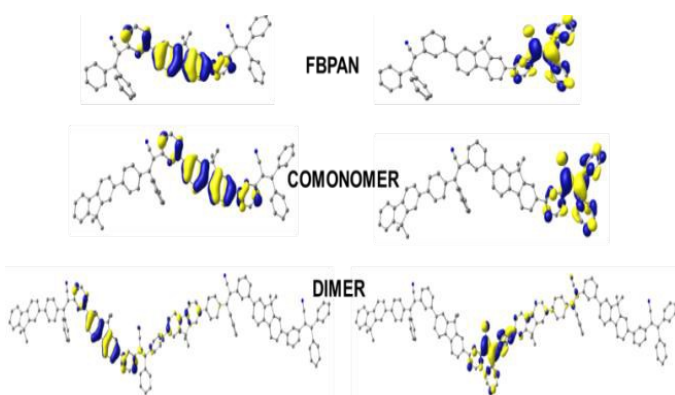


**Figure 12** Topologies of frontier molecular orbitals HOMO/LUMO (isosurface value = 0.03 au) of model co-polymers calculated at the B3LYP/6-31G\* level.

For the same system, the intramolecular charge transfer peak at located at 380 nm ( $f = 0.6923$ ). This transition arises from the  $H \rightarrow L$  and  $H \rightarrow L+1$ , respectively. In the case of dimer the maximum peak is predicted to be at 413 nm ( $f = 1.9268$ ) which arises from HOMO to LUMO (80%) transition.

#### Charge carrier mobility:

The hole and electron transport properties of the organic molecules can be explained using semi-classical Marcus theory, where the charge carrier motion occurs predominantly by a hop-ping-type mechanism.<sup>54,55</sup> It is clear from Marcus equation, the charge transfer rate depends upon two key parameters, the charge transfer integral (coupling matrix) and reorganization energy. The experimentally determined coupling matrix for organic molecules is however reported to be rather narrow. Hence, reorganization energy plays an important role when it comes to controlling hole and electron transfer rate, although such an assumption would be too simplistic. However, using this relation, reasonable correlations have been estimated between the molecular structure and charge transfer rate in organic materials.<sup>56-60</sup>

In order to evaluate the charge transport properties of the copolymer, the reorganization energies of the oligomer were evaluated. The reorganization energy is a qualitative indication of the charge-transport rate (the lower the reorganization energy value, the higher the charge transport rate). The reorganization energies were evaluated by the adiabatic potential-energy surface approach described in detail in previous studies.<sup>58,59</sup> The calculated hole ( $\lambda_h$ ) and electron ( $\lambda_e$ ) reorganization energies of FBPAN (dimer) are displayed in Table 2. It can be noticed from the results that the reorganization energy for hole transport ( $\lambda_h$ ) is lower than that for electron transport ( $\lambda_e$ ), which suggests that the hole transport performance of copolymer is more favorable than electron transport ability. However, difference between the  $\lambda_h$  and  $\lambda_e$  reorganization energies is comparable ( $\Delta\lambda = 0.12$  eV), which is sufficient<sup>60</sup> for them to act as good ambipolar charge carrier mobility. As a result, it may reduce the charge trapping pathways in the device.

**Table 2.** Calculated Hole ( $\lambda_h$ ) and Electron ( $\lambda_e$ ) Reorganization Energies of model polymer at B3LYP/6-31G\*Level (Energies in eV).

Compound	Hole			Electron		
	$\lambda_1$	$\lambda_2$	$\lambda_h$	$\lambda_3$	$\lambda_4$	$\lambda_e$
Dimer	0.04	0.03	0.07	0.09	0.10	0.19

#### Experimental section

<sup>1</sup>H and <sup>13</sup>C NMR spectra were recorded on a 400 MHz Bruker spectrophotometer using CDCl<sub>3</sub> ( $\delta = 7.26$  ppm) with tetramethylsilane (TMS,  $\delta = 0$ ) as internal standard. Mass spectra were taken on MALDI-mass Bruker ultraflex extreme spectrometer by using 4-HCCA ( $\alpha$ -Cyano-4-hydroxycinnamic acid) matrix. Elemental analysis was carried out using Euro Vector S.P.A, Euro EA 3000 CHNS elemental analyzer.

**Table 3** Summary of the excited state electronic transitions obtained from the TD-DFT calculations at the B3LYP/6-31G\* level

Model systems	States	Absorption (nm)	Energy (eV)	Oscillator strength ( <i>f</i> )	Dominant contribution <sup>a</sup> (%)	Exp. (nm)
FBPAN	S <sub>3</sub>	350	3.54	1.2629	H-1→L (82%), H→L+2(15%)	362
	S <sub>4</sub>	331	4.08	0.9764	H→L+2(81%), H-1→L (15%)	
	S <sub>7</sub>	300	4.14	0.3118	H-2→L+1 (84%)	
Monomer	S <sub>2</sub>	380	3.26	0.6923	H→L+1(66%), H-1→L+1(31%)	370
	S <sub>3</sub>	374	3.31	0.6494	H-1→L+1(66%), H→L+1(31%)	
	S <sub>5</sub>	349	3.55	0.9170	H-2→L (72%), H-1→L (13%)	
	S <sub>7</sub>	331	3.74	0.8395	H-2→L+1(95%)	
Dimer	S <sub>1</sub>	413	3.00	1.9268	H→L (80%), H-2→L (14%)	370
	S <sub>5</sub>	380	3.26	0.4870	H→L+2(29%), H-2→L+2(27%)	
	S <sub>7</sub>	374	3.31	0.6860	H-3→L+2(71%), H→L+2(16%)	

<sup>a</sup>H denotes HOMO and L denotes LUMO.

Fourier transform infrared (FT-IR) spectra of the compounds were recorded on an ABB BOMEM MB3000 spectrometer using KBr pellets. UV-visible absorbance spectra were done on Varian Carey 50 Bio UV-visible spectrophotometer. Fluorescence spectra of monomer and copolymers were recorded on Varian Carey Eclipse fluorescence spectrophotometer. Cyclic voltammetry measurements were done using CHI 600D electrochemical work stations with Ag/AgCl, platinum disc and platinum wire as reference, working, and counter electrodes respectively. Cyclic voltammetry were performed by coating a thin layer of polymers on platinum disc electrode and measurements were performed in acetonitrile medium with tetrabutylammonium hexafluorophosphate (0.1M ([Bu<sub>4</sub>N] PF<sub>6</sub>)) as support electrolyte. Dynamic light scattering (DLS) experiments of monomer and copolymers were performed on Malvern, DLS instrument. Fluorescence life time experiments were done on EDINBURGH (UK), FLS 980 TCSPC instruments. Atomic force micrographs (AFM) were obtained on RUSSIA model: NTEGRA PRIMA instrument at ambient conditions with NT-MDT solver software for analysis, Ireland. Scanning electron microscope (SEM) analyses were performed by Phenompro. Samples for AFM and SEM were prepared by spin coating 300 micro liter of the chloroform solution (2 mg ml<sup>-1</sup>) and over the surface area of 1.8 cm<sup>2</sup> of ITO coated glass substrate to simulate the end use device condition. Absolute quantum yield of electroluminescence for polymer was collected by measuring the total light output in all directions in an integrating sphere using EDINBURGH (UK), FLS 980 TCSPC instruments. GIXRD studies were performed on films of the polymers coated on ITO substrates using Bruker AX D8 advance X-ray diffractometer with Cu K $\alpha$  wave length of 1.5406 Å. Density functional theory (DFT) calculations were performed using B3LYP functional. The basis set used for the C, H, N atoms was 6-31 Gs. Details of theoretical calculations are provided in the supporting Information.

#### OLED fabrication and measurement

OLEDs of all the monomer and copolymers fabricated using indium tin oxide (ITO) with a sheet resistance 10Ω/square. The substrates were cleaned by a series of ultrasonic processing

with acetone, detergent, deionized water in an ultrasonic solvent path. After cleaned solvent bath and then baked in a heating chamber at 120°C and treated with oxygen plasma for 25 mins before use. The PEDOT-PSS (10-40 nm) solution was spin coated on cleaned ITO substrates and baked in a heating chamber at 200°C for one hour. After the above process 300 ml of polymer solutions with 1 mg/ml concentration in CHCl<sub>3</sub> were spin coated at 2000 rpm for 60 seconds to get uniform films of polymers (with thickness 100–150 nm) and the aluminium was coated at 105 Torr. Current–Voltage (I–V) characteristics were studied on a Keithley 2400 source meter. Luminescence–voltage (L–V) characteristics of the OLEDs were studied using NUCLEONIX type 168 PMT housing with drawer assembly. Electroluminescence spectra of the OLEDs were further measured using a Carey Eclipse fluorescence spectrophotometer. Commission Internationale de l’Eclairage (CIE) color coordinate values of the thin films of the LEDs were standardized using a Konica Minolta CS-100 Chroma meter in automated mode.

#### Conclusions

In conclusion, we introduced an effective approach for the rational design of white light emitting copolymer by incorporating strong AIEEgen as a dopant material. The white light emission is demonstrated, based on derivative of tetraphenylethene (FBPAN) building blocks alternating with 9,9'-dihexylfluorene core. The AIEE characteristics of FBPAN monomer showed absolute quantum yield of 63.4% in the solid state due to the restriction of intramolecular rotation owing to its twisted conformation. The AIEE active FBPAN rendered the copolymers improved AIEE performance and the copolymers exhibited enhanced emission even at very low feed ratios (0.5%) of AIEEgen compared to reported tetraphenylethylene-fluorene copolymers with 10% feed ratios.<sup>21</sup> The copolymer of FBPAN 0.5 elucidated a bright white light emission with absolute quantum yield as high as 80.2% due to the formation of “J-aggregates”, which control the unique order of flower shaped supramolecular self-assemblies in the solid state. The single active layer device of copolymer

FBPAN 0.5 showed pure white electroluminescence with CIE coordinates (0.32, 0.31), which are very close to those of standard white light emission (0.33, 0.33). The maximum luminance, current and power efficiency are 13455 cd/m<sup>2</sup>, 7.56 cd/A, 5.32 lm/W, respectively. The performance of our device is well comparable to that of white organic light emitting devices (WOLEDs) with multilayers and complicated fabrication processes.<sup>8</sup> From the device fabrication point of view, these copolymers provide significant advantage with the balanced charge transport due to the reduced energy offset. It is predicted that, based on our results the rational molecular design strategy can offer many new efficient light emitting materials for next generation.

## Acknowledgements

We are grateful to Dr Easwaramoorthy, Dr Aruna Dhathathreyan and J. Ajantha CSIR-CLRI, India for providing AFM, fluorescence lifetimes and absolute quantum yield studies. The timely help from Prof. R. Dhamodharan and Mr. E. Ramachandran, department of chemistry, IIT Madras is gratefully acknowledged. The authors gratefully acknowledge the financial support from CSIR-TAPSUN (NWP-0055). The author, E. Ravindran thanks to CSIR for providing the senior research fellowship (Grant No. 31/6(398)/2014-EMR-I).

## Notes and references

- (a) C. W. Tang and S. A. VanSlyke, *Appl. Phys. Lett.*, 1987, **51**, 93; (b) Y. Hong, J. W. Y. Lam and B. Z. Tang, *Chem. Soc. Rev.*, 2011, **40**, 5361; (c) F. Wurthner, T. E. Kaiser and C. R. Saha-Mçller, *Angew. Chem. Int. Ed.*, 2011, **123**, 3436; (d) W. Wu, R. Tang, Q. Li and Zhen Li, *Chem. Soc. Rev.*, 2015, **44**, 3997.
- (a) B. W. D'Andrade and S. R. Forrest, *Adv. Mater.*, 2004, **16**, 1585; (b) Y. Sun, N. C. Giebink, H. Kanno, B. Ma, M. E. Thompson and S. R. Forrest, *Nature*, 2006, **440**, 908; (c) A. Misra, P. Kumar, M. N. Kamalasanan and S. Chandra, *Semicond. Sci. Technol.*, 2006, **21**, R35; (d) H. B. Wu, L. Ying, W. Yang and Y. Cao, *Chem. Soc. Rev.*, 2009, **38**, 3391; (e) X. Yang, G. Zhou and W.-Y. Wong, *J. Mater. Chem. C*, 2014, **2**, 1760.
- (a) L. X. Wang, X. B. Jing and F. S. Wang, *Acta Polym. Si.*, 2009, **10**, 980; (b) G. M. Farinola and R. Ragni, *Chem. Soc. Rev.*, 2011, **40**, 3467; (c) M. C. Gather, A. Kohnen and K. Meerholz, *Adv. Mater.*, 2011, **23**, 233; (d) K. T. Kamtekar, A. P. Monkman and M. R. Bryce, *Adv. Mater.*, 2010, **22**, 572; (e) S. Beaupre, P. L. T. Boudreaux and M. Leclerc, *Adv. Mater.*, 2010, **22**, E6; (f) H. Sasabe and J. Kido, *J. Mater. Chem. C*, 2013, **1**, 1699.
- (a) S. Reineke, F. Lindner, G. Schwartz, N. Seidler, K. Walzer, B. Lüssem and K. Leo, *Nature*, 2009, **459**, 234; (b) J. Kido, M. Kimura and K. Nagai, *Science*, 1995, **267**, 1332; (c) W. Y. Wong and C. L. Ho, *J. Mater. Chem.*, 2009, **19**, 4457; (d) Z. Xie, C. Chen, S. Xu, J. Li, Y. Zhang, S. Liu, J. Xu, and Z. Chi *Angew. Chem. Int. Ed.*, 2015, **54**, 7181.
- (a) H. Wu, L. Ying, W. Yang and Y. Cao, *Chem. Soc. Rev.*, 2009, **38**, 3391; (b) K. T. Kamtekar, A. P. Monkman and M. R. Bryce, *Adv. Mater.*, 2010, **22**, 572.
- (a) T.-H. Kim, H. K. Lee, O. O. Park, B. D. Chin, S.-H. Lee and J. K. Kim, *Adv. Funct. Mater.*, 2006, **16**, 611; (b) P.-I. Shih, Y.-H. Tseng, F.-I. Wu, A. K. Dixit and C.-F. Shu, *Adv. Funct. Mater.*, 2006, **16**, 1582; (c) X. Gong, W. Ma, J. C. Ostrowski, G. C. Bazan, D. Moses and A. J. Heeger, *Adv. Mater.*, 2004, **16**, 615; (d) J. Huang, G. Li, E. Wu, Q. Xu and Y. Yang, *Adv. Mater.*, 2006, **18**, 114; (d) J. Huang, W.-J. Hou, J.-H. Li, G. Li and Y. Yang, *Appl. Phys. Lett.*, 2006, **89**, 133509.
- (a) S. Tasch, E. J. W. List, O. Ekstrom, W. Graupner, G. Leising, P. Schlichting, U. Rohr, Y. Geerts, U. Scherf and K. Müllen, *Appl. Phys. Lett.*, 1997, **71**, 2883; (b) X. Gong, S. Wang, D. Moses, G. C. Bazan and A. J. Heeger, *Adv. Mater.*, 2005, **17**, 2053.
- (a) A. Garcia, R. Yang, Y. Jin, B. Walker and T. Q. Nguyen, *Appl. Phys. Lett.*, 2007, **91**, 153502; (b) B. W. D'Andrade and S. R. Forrest, *Adv. Mater.*, 2004, **16**, 1585; (c) S. Chen, Q. Wu, M. Kong, X. Zhao, Z. Yu, P. Jiaa and W. Huang, *J. Mater. Chem. C*, 2013, **1**, 3508.
- (a) R. S. Deshpandae, V. Bulovic and S. R. Forrest, *App. Phys. Lett.*, 1999, **75**, 888; (b) L. Zhang, S. Hu, J. Chen, Z. Chen, H. Wu, J. Peng and Y. Cao, *Adv. Funct. Mater.*, 2011, **21**, 3760.
- (a) E. Ravindran, S. J. Ananthakrishnan, E. Varathan, V. Subramanian and N. Somanathan, *J. Mater. Chem. C*, 2015, **3**, 4359; (b) S. J. Ananthakrishnan, E. Varathan, V. Subramanian, N. Somanathan and A. B. Mandal, *J. Phys. Chem. C*, 2014, **118**, 084; (c) S. J. Ananthakrishnan, E. Varathan, N. Somanathan, V. Subramanian, A. B. Mandal, J. D. Sudha and R. Ramakrishnan, *J. Mater. Chem. C*, 2014, **2**, 9035.
- (a) L. Chen, Y. Jiang, H. Nie, P. Lu, H. H. Y. Sung, I. D. Williams, H. S. Kwok, F. Huang, A. Qin, Z. Zhao and B. Z. Tang, *Adv. Funct. Mater.*, 2014, **24**, 3621; (b) J. Huang, N. Sun, J. Yang, R. Tang, Q. Li, D. Ma and Z. Li, *Adv. Funct. Mater.*, 2014, **24**, 7645; (c) G. Mu, W. Zhang, P. Xu, H. Wang, Y. Wang, L. Wang, S. Zhuang and X. Zhu, *J. Phys. Chem. C*, 2014, **118**, 8610.
- (a) J. Luo, Z. Xie, J. W. Y. Lam, L. Cheng, H. Chen, C. Qiu, H. S. Kwok, X. Zhan, Y. Liu, D. Zhu and B. Z. Tang, *Chem. Commun.*, 2001, 1740; (b) S. W. Thomas, G. D. Joly and T. M. Swager *Chem. Rev.*, 2007, **107**, 1339; (c) B. K. An, S. K. Kwon, S. D. Jung and S. Y. Park, *J. Am. Chem. Soc.*, 2002, **124**, 14410.
- (a) Z. Li, Y. Q. Dong, J. W. Y. Lam, J. Sun, A. Qin, M. Ha'ußler, Y. P. Dong, H. H. Y. Sung, I. D. Williams, H. S. Kwok and B. Z. Tang, *Adv. Funct. Mater.*, 2009, **19**, 905. (b) J. W. Chen, H. Peng, C. C. W. Law, Y. P. Dong, J. W. Y. Lam, I. D. Williams and B. Z. Tang, *Macromolecules*, 2003, **6**, 4319; (c) J. W. Chen, B. Xu, X. Y. Ouyang, B. Z. Tang and Y. Cao, *J. Phys. Chem. A*, 2004, **108**, 7522; (d) J. W. Chen, C. C. W. Law, J. W. Y. Lam, Y. P. Dong, S. M. F. Lo, I. D. Williams, D. B. Zhu and B. Z. Tang, *Chem. Mater.*, 2003, **15**, 1535.
- (a) H. Tong, Y. Q. Dong, M. Haussler, J. W. Y. Lam, H. H. Y. Sung, I. D. Williams, J. Z. Sun and B. Z. Tang, *Chem. Commun.*, 2006, 1133; (b) A. J. Qin, C. K. W. Jim, Y. H. Tang, J. W. Y. Lam, J. Z. Liu, F. Mahtab, P. Gao and B. Z. Tang, *J. Phys. Chem. B*, 2008, **112**, 9281.
- (a) Y. P. Li, F. Li, H. Y. Zhang, Z. Q. Xie, W. J. Xie, H. Xu, B. Li, F. Z. Shen, L. Ye, M. Hanif, D. G. Ma and Y. G. Ma, *Chem. Commun.*, 2007, 231; (b) C. Deng, Y. Niu, Q. Peng, A. in, Z. Shuai and B. Z. Tang, *J. Chem. Phys.*, 2011, **135**, 014304.
- Y. Qian, M. M. Cai, L. H. Xie, G. Q. Yang, S. K. Wu and W. Huang, *Chem Phys Chem*, 2011, **12**, 397.
- R.-H. Chien, C.-T. Lai and J.-L. Hong, *J. Phys. Chem. C*, 2011, **115**, 12358.
- J.-F. Lamere, N. Saffon, I. Dos Santos and S. Fery-Forgues, *Langmuir*, 2010, **26**, 10210.
- Y. Liu, Y. Yu, J. W. Y. Lam, Y. Hong, M. Faisal, W. Z. Yuan and B. Z. Tang, *Chem. Eur. J.*, 2010, **16**, 8433.
- (a) J. Mei, N. L. C. Leung, R. T. K. Kwok, J. W. Y. Lam and B. Z. Tang, *Chem. Rev.*, 2015, **115** (21), 11718; (b) S.-J. Yoon, J. W. Chung, J. Gierschner, K. S. Kim, M.-G. Choi, D. Kim and S. Y. Park, *J. Am. Chem. Soc.*, 2010, **132**, 13675; (c) Z. Y. Zhang, B. Xu, J. H. Su, L. P. hen, Y. S. Xie and H. Tian, *Angew. Chem., Int.*

- Ed*, 2011, **50**, 11654; (d) C. L. Tan, X. Y. Qi, X. Huang, J. Yang, B. Zheng, Z. F. An, R. F. Chen, J. Wei, B. Z. Tang, W. Huang and H. Zhang, *Adv. Mater.*, 2014, **26**, 1735.
- 21 (a) Y. Dong, J. W. Y. Lam, A. Qin, J. Liu, Z. Li, B. Z. Tang, J. Sun and H. S. Kwok, *Appl. Phys. Lett.*, 2007, **91**, 011111; (b) Z. Zhao, S. Chen, X. Shen, F. Mahtab, Y. Yu, P. Lu, J. W. Y. Lam, H. S. Kwok and B. Z. Tang, *Chem. Commun* 2010, **46**, 686; (c) J. Wang, J. Mei, R. R. Hu, J. Z. Sun, A. J. Qin and B. Z. Tang, *J. Am. Chem. Soc.*, 2012, **134**, 9956; (d) W.-L. Gong, B. Wang, M. P. Aldred, C. Li, G.-F. Zhang, T. Chen, L. Wang and M.-Q. Zhu, *J. Mater. Chem. C*, 2014, **2**, 7001.
- 22 J. Shi, Y. Wu, S. Sun, B. Tong, J. Zhi and Y. Dong, *Journal Of Polymer Science Part A: Polymer Chemistry*, 2013, **51**, 229.
- 23 S. M. King, I. I. Perepichka, I. F. Perepichka, F. B. Dias, M. R. Bryce and A. P. Monkman, *Adv. Funct. Mater.*, 2009, **19**, 586.
- 24 (a) J. L. S. Shao, L. Chen, Z. Xie, Y. Cheng, Y. Geng, L. Wang, X. Jing, and F. Wang, *Adv. Mater.*, 2007, **19**, 1859; (b) Y. Zhang, H. Li, G. Zhang, X. Xu, L. Kong, X. Tao, Y. Tian and J. Yang, *J. Mater. Chem. C*, 2016, **4**, 2971.
- 25 (a) J. Luo, X. Li, Q. Hou, J. Peng, W. Yang and Y. Cao, *Adv. Mater.*, 2007, **19**, 1113; (b) C.-Y. Sun, X.-L. Wang, X. Zhang, C. Qin, P. Li, Z.-M. Su, D.-X. Zhu, G.-G. Shan, K.-Z. Shao, H. Wu and J. Li, *Nat. Commun*, 2013, **4**, 2717.
- 26 (a) S. W. Thomas, G. D. Joly and T. M. Swager, *Chem. Rev.*, 2007, **107**, 1339; (b) Z. J. Ning, Z. Chen, Q. Zhang, Y. L. Yan, S. X. Qian, Y. Cao and H. Tian, *Adv. Funct. Mater.*, 2007, **17**, 3799; (c) H. N. Kim, Z. Guo, W. Zhu, J. Yoon and H. Tian, *Chem. Soc. Rev.*, 2011, **40**, 79; (d) Y. Hong, L. Meng, S. Chen, C. W. T. Leung, L. Da, M. Faisal, D.-A. Silva, J. Liu, J. W. Y. Lam, X. Huang and B. Z. Tang, *J. Am. Chem. Soc.*, 2012, **134**, 1680.
- 27 (a) Y. Dong, J. W. Y. Lam, A. Qin, J. Sun, J. Liu, Z. Li, J. Sun, H. H. Y. Sung, I. D. Williams, H. S. Kwok and B. Z. Tang, *Chem. Commun*, 2007, 3255; (b) Z. Zhao, Z. Wang, P. Lu, C. Y. K. Chan, D. Liu, J. W. Y. Lam, H. H. Y. Sung, I. D. Williams, Y. Ma and B. Z. Tang, *Angew. Chem., Int. Ed.*, 2009, **48**, 7608; (c) Y. Cai, K. Samedov, H. Albright, B. S. Dolinar, I. A. Guzei, R. Hu, C. Zhang, B. Z. Tang and R. West, *Chem. Commun*, 2014, **50**, 12714; (d) L. C. Palilis, A. J. Mäkinen, M. Uchida and Z. H. Kafafi, *Appl. Phys. Lett.*, 2003, **82**, 2209.
- 28 (a) J. Mei, Y. Hong, J. W. Y. Lam, A. Qin, Y. Tang and B. Z. Tang, *Adv. Mater.*, 2014, **26**, 5429; (b) Z. He, L. Shan, J. Mei, H. Wang, J. W. Y. Lam, H. H. Y. Sung, I. D. Williams, X. Gu, Q. Miao and B. Z. Tang, *Chem. Sci.*, 2015, **6**, 3538.
- 29 (a) B. K. An, S. K. Kwon, S. D. Jung and S. Y. Park, *J. Am. Chem. Soc.*, 2002, **124**, 14410; (b) J. Xu, L. Wen, W. Zhou, J. Lv, Y. Guo, M. Zhu, H. Liu, Y. Li and L. Jiang, *J. Phys. Chem. C*, 2009, **113**, 5924; (c) S. Jayanty and T. P. Radhakrishnan, *Chem. Eur. J.*, 2004, **10**, 791.
- 30 (a) W. Z. Yuan, Y. Gong, S. Chen, X. Y. Shen, J. Y. Y. Lam, P. Lu, Y. Lu, Z. Wang, R. Hu, N. Xie, H. Kwok, Y. Zhang, J. Z. Sun, and B. Z. Tang, *Chem. Mater.*, 2012, **24**, 1518; (b) M. R. Bryce, *Adv. Mater.*, 1999, **11**, 11; (c) Z. R. Grabowski and K. Rotkiewicz, *Chem. Rev.*, 2003, **103**, 3899; (d) E. Ahmed, S. Subramaniyan, F. S. Kim, H. Xin and S. A. Jenekhe, *Macromolecules*, 2011, **44**, 7207; (e) T.-C. Lin, G. S. He, Q. Zheng, P. N. Prasad, *J. Mater. Chem.*, 2006, **16**, 2490.
- 31 (a) Q. Q. Li, J. H. Zou, J. W. Chen, Z. J. Liu, J. G. Qin, Z. Li and Y. Cao, *J. Phys. Chem. B*, 2009, **113**, 5816; (b) M. P. Aldred, C. Li, G. F. Zhang, W. L. Gong, A. D. Q. Li, Y. D. D. Ma and M. Q. Zhu *J. Mater. Chem.*, 2012, **22**, 7515.
- 32 (a) Z. Zhao, J. W. Y. Lam and B. Z. Tang, *J. Mater. Chem.*, 2012, **22**, 23726;
- 33 (a) X. Yao, X. Ma and H. Tian, *J. Mater. Chem. C*, 2014, **2**, 5155; (b) L. M. Ilharco and R. Brito de Barros, *Langmuir*, 2000, **16**, 9331; (c) Z. Zhao, P. Lu, J. W. Y. Lam, Z. Wang, C. Y. K. Chan, H. H. Y. Sung, I. D. Williams, Y. Mab and B. Z. Tang, *Chem. Sci.*, 2011, **2**, 672.
- 34 (a) S. J. Ananthkrishnan, E. Varathan, E. Ravindran, N. Somanathan, V. Subramanian, A. B. Mandal, J. D. Sudha and R. Ramakrishnan, *Chem. Commun*, 2013, **49**, 10742.
- 35 (a) J. Yang, J. Huang, Q. Li and Z. Li, *J. Mater. Chem. C*, 2016, **4**, 2663; (b) Y. Hong, J. W. Y. Lam, and B. Z. Tang, *Chem. Commun*, 2009, 4332; (c) Y. Hong, J. W. Y. Lam and B. Z. Tang, *Chem. Soc. Rev.*, 2011, **40**, 5361; (d) Z. Zhao, J. W. Y. Lam and B. Z. Tang, *Curr. Org. Chem.*, 2010, **14**, 2109; (e) W. Z. Yuan, H. Zhao, X. Y. Shen, F. Mahtab, J. W. Y. Lam, J. Z. Sun and B. Z. Tang, *Macromolecules*, 2009, **42**, 9400.
- 36 F. Würthner, T. E. Kaiser and C. R. Saha-Möllner, *Angew. Chem. Int. Ed.*, 2011, **50**, 3376.
- 37 (a) G. Seelig, D. Soloveichik, D. Y. Zhang and E. Winfree, *Science*, 2006, **314**, 1585; (b) K. S. Park, M. W. Seo, C. Jung, J. Y. Lee and H. G. Park, *Small*, 2012, **8**, 2203.
- 38 (a) P. Gale and J. Steed *Supramolecular Chemistry: From Molecules to Nanomaterials*, ed., Wiley-VCH Verlag GmbH & Co. KGaA, Weinheim, 2012; (b) E. Busseron, Y. Ruff, E. Moulin and N. Giuseppone, *Nanoscale*, 2013, **5**, 7098.
- 39 (a) F. M. Menger, *Proc. Natl. Acad. Sci. U. S. A.*, 2002, **99**, 4818; (b) J.-M. Lehn, *Proc. Natl. Acad. Sci. U. S. A.*, 2002, **99**, 4763.
- 40 (a) J. M. Zayed, N. Nouvel, U. Rauwald and O. A. Scherman, *Chem. Soc. Rev.*, 2010, **39**, 2806; (b) C. Wang, Z. Wang and X. Zhang, *Acc. Chem. Res.*, 2012, **45**, 608; (c) B. Rybtchinski, *ACS Nano*, 2011, **5**, 6791.
- 41 (a) U. Shinya, M. Takehiko and T. Toshihiro, *Sci. Technol. Adv. Mater.*, 2009, **10**, 020301; (b) Y. Yamamoto, *Sci. Technol. Adv. Mater.*, 2012, **13**, 33001; (c) E. Moulin, J.-J. Cid and N. Giuseppone, *Adv. Mater.*, 2013, **25**, 477; (d) S. S. Babu, S. Prasanthkumar and A. Ajayaghosh, *Angew. Chem., Int. Ed.*, 2012, **51**, 1766; (e) M. Hasegawa and M. Iyoda, *Chem. Soc. Re.*, 2010, **39**, 2420.
- 42 N. Delbosc, M. Reynes, O. J. Dautel, G. Wantz, J.-P. Lere-Porte and J. J. E. Moreau, *Chem. Mater.*, 2010, **22**, 18.
- 43 A. K. Boal, F. Ilhan, J. E. DeRouchey, T. T. Albrecht, T. P. Russell and V. M. Rotello, *Nature*, 2000, **404**, 746.
- 44 S. I. Stupp and L. C. Palmer *Chem. Mater.*, 2014, **26**, 507.
- 45 S. Kawana, M. Durrell, J. Lu, J. E. Macdonald, M. Grell, D. D. C. Bradley, P. C. Jukes, R. A. L. Jones and S. L. Bennett, *Polymer*, 2002, **43**, 1907.
- 46 S. K. Lee, T. Ahn, J.-H. Park, Y. K. Jung, D.-S. Chung, C. E. Parke and H. K. Shim, *J. Mater. Chem.*, 2009, **19**, 7062.
- 47 A. J. Cadby, P. A. Lane, H. Mellor, S. J. Martin, M. Grell, C. Giebeler and D. D. C. Bradley, *Phys Rev B*, 2000, **62**, 15604.
- 48 J. M. Mazzeo, D. Pisignano, F. Dellasala, J. Thompson, R. I. R. Blyth, G. Gigli, R. Cingolani, G. Sotgiu and G. Barbarella *Appl. Phys. Lett.*, 2003, **82**, 334.
- 49 (a) J. Liu, Q. Zhou, Y. Cheng, Y. Geng, L. Wang, D. zMa, X. Jing, F. Wang, *Adv. Mater.*, 2005, **17**, 2974; (b) C-Y Chuang, P-I. Shih, C-H. Chien, F-I. Wu and C-F Shu, *Macromolecules*, 2007, **40**, 247.
- 50 (a) J. Liu, Q. Zhou, Y. Cheng, Y. Geng, L. Wang, D. Ma, X. Jing and F. Wang, *Adv. Funct. Mater.*, 2006, **16**, 957; (b) B. Zhang, C. Qin, J. Ding, L. Chen, Z. Xie, Y. Cheng and L. Wang, *Adv. Funct. Mater.*, 2010, **20**, 295.
- 51 J. Lee, J. I. Lee, M. J. Park, Y. K. Jung, N. S. Cho, H. J. Cho, D. H. Hwang, S. K. Lee, J. H. Park, J. Hong, H. Y. Chu and H. K. Shim, *J. Polym. Sci, Part A: Polym. Chem*, 2007, **45**, 1236.
- 52 S. P. Singh, Y. N. Mohapatra, M. Qureshi, S. S. Manoharan, *Appl. Phys. Lett.* 2005, **86**, 113505/1.
- 53 L. Chen, P. C. Li, Y. X. Cheng, Z. Y. Xie, L. X. Wang, X. B. Jing and F. S. Wang, *Adv. Mater.*, 2011, **23**, 2986.
- 54 V. Coropceanu, J. Cornil, D. A. da Silva Filho, Y. Olivier, R. Silbey and J.-L. Brédas, *Chem. Rev.* 2007, **107**, 926.
- 55 R. A. Marcus, *J. Chem. Phys.*, 1956, **24**, 966.
- 56 X. Q. Ran, J. K. Feng, A. M. Ren, W. C. Li, L. Y. Zou and C. C. J. Sun, *Phys. Chem. A*, 2009, **113**, 7933.

## ARTICLE

Journal Name

- 57 G. R. Hutchison, M. A. Ratner and T. J. J. Marks, *Am. Chem. Soc.*, 2005, **127**, 2339.
- 58 E. Varathan, D. Vijay, P. S. Vinod Kumar and V. Subramanian, *J. Mater. Chem. C*, 2013, **1**, 4261.
- 59 E. Varathan, D. Vijay and V. Subramanian, *J. Phys. Chem. C*, 2014, **118**, 21741.
- 60 J. Yin, S.-L. Zhang, R.-F. Chen, Q.-D. Ling and W. Huang, *Phys. Chem. Chem. Phys.* 2010, **12**, 15448.

## Graphical Abstract

Aggregation-induced emission enhancement (AIEE) offers solution to the problem of aggregation caused quenching (ACQ) in solid state; the rational molecular designing of AIEE strategy can offer many new efficient light emitting materials.

